

Quest for the dynamics of $\nu_\mu \rightarrow \nu_\tau$ conversion

A. M. Gago,^{1,2,*} E. M. Santos,^{1,†} W. J. C. Teves,^{1,‡} and R. Zukanovich Funchal^{1,§}

¹*Instituto de Física, Universidade de São Paulo, C.P. 66.318, 05315-970 São Paulo, Brazil*

²*Sección Física, Departamento de Ciencias, Pontificia Universidad Católica del Perú, Apartado 1761 Lima, Perú*

(Received 10 October 2000; published 3 May 2001)

We perform a quantitative analysis of the capability of K2K, MINOS, OPERA, and a neutrino factory in a muon collider to discriminate the standard mass induced vacuum oscillation from the pure decoherence solution to the atmospheric neutrino problem and thereby contribute to unravel the dynamics that governs the observed ν_μ disappearance.

DOI: 10.1103/PhysRevD.63.113013

PACS number(s): 14.60.Pq

I. INTRODUCTION

Two years ago, the Super-Kamiokande (SuperK) atmospheric neutrino data astonished the world by giving the first compelling evidence in favor of $\nu_\mu \rightarrow \nu_\tau$ oscillations [1]. This incredible result has since been confirmed by other atmospheric neutrino experiments [2,3], as well as by the preliminary K2K ν_μ disappearance experiment result [4], making unquestionable the fact that neutrinos suffer flavor conversion.

Naively, one may think that proves neutrinos have non-zero mass and that the next challenge for experimentalists is simply to determine the neutrino mass squared differences and the texture of the neutrino mixing matrix. Indeed, if the dynamics of neutrino flavor change is mass induced in the standard way [5], this is obviously the next logical step. Unfortunately, this is not an established fact.

Although the atmospheric neutrino data collected up to now allow one to definitely exclude some energy dependences for the $\nu_\mu \rightarrow \nu_\tau$ conversion probability [6], some interesting possibilities, such as neutrino decay [7] and pure quantum decoherence [8], are capable of explaining the data comparably well in light of the standard mass induced oscillation mechanism. This is in spite of the fact that the dynamics behind neutrino decay and pure decoherence gives rise to a ν_μ survival probability monotonically decreasing with neutrino energy while the mass induced mechanism leads to a harmonic probability of oscillation. We therefore believe that another important experimental task should be to unravel the nature of the flavor changing mechanism. We have to point out that the neutrino decay scenario is also mass induced, but throughout this paper when we allude to the mass induced mechanism, we will be referring to the standard neutrino flavor oscillation scenario.

Many, if not all, of the proposed future neutrino long-base-line experiments were designed to measure $\nu_\mu \rightarrow \nu_\tau$ oscillations in order to pin down the oscillation parameters having in mind the standard mass induced oscillation mechanism. It is important to verify their real capabilities to dis-

criminate among different flavor changing dynamics.

The purpose of this paper is to investigate to what extent K2K and the next generation neutrino oscillation experiments will be able to discriminate the mass induced $\nu_\mu \rightarrow \nu_\tau$ oscillation solution [9] to the atmospheric neutrino problem (ANP) from the recently proposed pure decoherence one [8]. We do not investigate in this paper the decay mechanism, since it implies the existence of sterile neutrinos, giving rise to a richer phenomenology; this study will be reported elsewhere [10].

The outline of the paper is as follows. In Sec. II, we briefly review the mass induced and the pure decoherence mechanisms of flavor conversion. In Sec. III, we define the statistical significance tests we will use in order to quantify the separation between the two ANP solutions. In Sec. IV, we discuss the power of discrimination of the mass induced oscillation solution to the ANP from the dissipative one at K2K [11], MINOS [12], OPERA [13], and a possible neutrino factory in a muon collider [14]. Finally, in Sec. V, we present our conclusions.

II. REVIEW OF THE FORMALISM

The time evolution of neutrinos created at a given flavor ν_μ by weak interactions, as of any quantum state, can be described using the density matrix formalism by the Liouville equation [15]. If we add an extra term $L[\rho_\mu]$ to the Liouville equation, quantum states can develop dissipation and irreversibility [15,16]. The generalized Liouville equation for $\rho_\mu(t)$ can then be written as [15]

$$\frac{d\rho_\mu(t)}{dt} = -i[H, \rho_\mu(t)] + L[\rho_\mu(t)], \quad (1)$$

where the effective Hamiltonian H is, in vacuum, given by

$$H = \begin{bmatrix} \Delta & 0 \\ 0 & -\Delta \end{bmatrix}, \quad (2)$$

where $\Delta = (m_2^2 - m_1^2)/4E_\nu$. We have already considered ultrarelativistic neutrinos of energy E_ν and the irrelevant global phase has been subtracted out. We assume here oscillations only between ν_μ and ν_τ in a two-generation scheme.

The most general parametrization for $L[\rho]$ contains six real parameters which are not independent if one assumes the

*Email address: agago@charme.if.usp.br

†Email address: emoura@charme.if.usp.br

‡Email address: teves@charme.if.usp.br

§Email address: zukanov@charme.if.usp.br

complete positivity condition [15]. In one of the simplest situations, which in fact physically arises when the weak coupling limit condition is satisfied, only one of the parameters, γ , has to be considered. In this limit, Eq. (1) can be solved to calculate [15]

$$P(\nu_\mu \rightarrow \nu_\tau) = \frac{1}{2} \sin^2 2\theta [1 - e^{-2\gamma L} \cos(2\Delta L)], \quad (3)$$

the probability of finding the neutrino produced in the flavor state ν_μ in the flavor state ν_τ after traveling a distance L under the influence of quantum dissipation driven by the parameter γ .

When $\gamma=0$, we get the usual mass induced oscillation (MIO) probability in two generations. The survival probability, in this case, is the standard one:

$$P(\nu_\mu \rightarrow \nu_\tau) = \frac{1}{2} \sin^2 2\theta [1 - \cos(2\Delta L)]. \quad (4)$$

On the other hand, if neutrinos are massless or degenerate ($\Delta m^2=0$) and weak interaction eigenstates are equal to mass eigenstates, even though standard oscillations cannot occur, flavor conversion can still take place through the pure decoherence mechanism (PDM) [17]. Explicitly, the neutrino flavor change probability, in the simplest case where a single decoherence parameter is considered, becomes

$$P(\nu_\mu \rightarrow \nu_\tau) = \frac{1}{2} [1 - e^{-2\gamma L}]. \quad (5)$$

We will assume here for the PDM that $\gamma = \gamma_0(E_\nu/\text{GeV})^{-1}$, where γ_0 is a constant given in GeV. This ansatz may be motivated by the assumption that the exponent in Eq. (5) behaves like a scalar under Lorentz transformations [8].

Note that here we will be studying both MIOs and the PDM in a two-generation framework since this is enough to explain well the atmospheric neutrino data. Notwithstanding, one may wonder about the contribution from electron neutrinos. If the PDM really takes place in nature, it should in fact involve all three neutrino flavors. We can have some insight into what can happen in this case. From the results of Refs. [17,18] on the limits on the PDM from SN 1987A data and with the ansatz above, we expect the decoherence parameter that accompanies the $\nu_\mu \rightarrow \nu_e$ conversion to be smaller than 10^{-39} GeV. This means that for the energies and distances of the long-base-line experiments we will study here, this effect should be completely negligible. Nevertheless, a complete study of the PDM with three neutrino generations should in fact be performed to confirm this assumption.

III. STATISTICAL SIGNIFICANCE TEST

In order to define the capability of an experiment to discriminate mass induced $\nu_\mu \rightarrow \nu_\tau$ oscillation from pure decoherence, we define the number of standard deviations of separation between MIOs and the PDM as $n_\sigma = \sqrt{\chi^2}$ where

$$\begin{aligned} \chi^2(\gamma_0, \sin^2 2\theta, \Delta m^2) = & 2[N^{\text{PDM}}(\gamma_0) - N^{\text{MIO}}(\sin^2 2\theta, \Delta m^2)] \\ & + 2N^{\text{MIO}}(\sin^2 2\theta, \Delta m^2) \\ & \times \ln \left(\frac{N^{\text{MIO}}(\sin^2 2\theta, \Delta m^2)}{N^{\text{PDM}}(\gamma_0)} \right) \end{aligned} \quad (6)$$

is the confidence level according to the procedure proposed by the Particle Data Group [19]. Here, $N^{\text{PDM}}(\gamma_0)$ is the total number of events theoretically expected if the PDM is the solution to the ANP and $N^{\text{MIO}}(\sin^2 2\theta, \Delta m^2)$ is the total number of events that can be observed by the experiment as a function of the two parameters involved in the MIO mechanism.

For each experiment we have studied, we have computed two different types of contour level curves.

First, we fix $N^{\text{PDM}} = N^{\text{PDM}}(\gamma_0^{\text{best}})$, at the number corresponding to $\gamma_0 = \gamma_0^{\text{best}} = 0.6 \times 10^{-21}$ GeV, the best-fit point of the PDM solution to the ANP [8], and vary the MIO parameters in the interval $1 \times 10^{-3} \text{ eV}^2 \leq \Delta m^2 \leq 2 \times 10^{-2} \text{ eV}^2$ and $0.8 \leq \sin^2 2\theta \leq 1$, consistent with the atmospheric neutrino data. In this way, we obtain curves of fixed n_σ in the plane $\sin^2 2\theta \times \Delta m^2$.

Second, we fix $\sin^2 2\theta = 1$ and vary the PDM parameter γ_0 in the interval $0.25 \times 10^{-21} \text{ GeV} \leq \gamma_0 \leq 1.1 \times 10^{-21} \text{ GeV}$, as well as the MIO parameter Δm^2 in the interval $1 \times 10^{-3} \text{ eV}^2 \leq \Delta m^2 \leq 2 \times 10^{-2} \text{ eV}^2$. The upper limit of the range in γ_0 is the one allowed by the CHORUS and NOMAD data [8,17]; the lower limit was estimated by using $\gamma_0 \sim 2.54 \times 10^{-19} \times (\Delta m^2/\text{eV}^2)$ GeV, with $\Delta m^2 = 1.0 \times 10^{-3} \text{ eV}^2$. Like this, we can get curves of fixed n_σ in the plane $\gamma_0 \times \Delta m^2$. This allows us to extend our conclusions beyond the best-fit value of the PDM solution to the ANP.

IV. PDM VERSUS MIO

We have investigated the capability of K2K [11,20,21] and the next generation neutrino oscillation experiments MINOS [12], OPERA [13,22], and a neutrino factory in a muon collider [14] to discriminate the PDM solution to the ANP with $\gamma_0 \sim 0.6 \times 10^{-21}$ GeV,¹ using the ansatz $\gamma = \gamma_0(E_\nu/\text{GeV})^{-1}$, given in Ref. [8], from the traditional one due to $\nu_\mu \rightarrow \nu_\tau$ MIOs in vacuum with $\Delta m^2 \sim (1.1-7.8) \times 10^{-3} \text{ eV}^2$ and $\sin^2 2\theta \gtrsim 0.84$ [9]. We recall that the best-fit point for the MIO solution to the ANP is at $(\sin^2 2\theta, \Delta m^2) = (1.0, 3.0 \times 10^{-3} \text{ eV}^2)$ [9].

We would like to point out that the decoherence solution to the ANP is open to two different readings: either it can be viewed as an effect of pure decoherence or as a combination of quantum decoherence plus vacuum oscillation driven by $\Delta m^2 \lesssim 10^{-6} \text{ eV}^2$ with $\sin^2 2\theta \sim 1$. In the first case, there is a single free parameter (γ_0) and the flavor change probability is given by Eq. (5); in the second, there are two free param-

¹We remark that in our notation $2\gamma_0$ corresponds to γ_0 of Ref. [8].

eters (γ_0 and $\sin^2 2\theta$) since the probability will be given by Eq. (3) with $\cos(2\Delta L) \rightarrow 1$.

We now present and discuss the results of our study.

A. K2K

In Ref. [8], K2K was cited as a possible experiment to test the novel decoherence solution to the ANP. This possibility would be very appealing for K2K is an experiment which is currently taking data.

In order to verify this, we have calculated the expected number of events in K2K for the goal of the experiment, i.e., 10^{20} protons on target (POT) [4], for three hypotheses: no flavor conversion, mass induced $\nu_\mu \rightarrow \nu_\tau$ oscillation with parameters consistent with SuperK atmospheric neutrino results [9], and the pure decoherence solution to the ANP [8].

K2K is a $\nu_\mu \rightarrow \nu_\mu$ disappearance experiment, where the muon neutrinos that have an average energy of 1.4 GeV are produced by the KEK accelerator, first measured after traveling 300 m by the Near Detector, which is a 1 kton water Cherenkov detector, and finally measured by the Far Detector (FD), the SuperK 22.5 kton water Cherenkov detector localized at 250 km from the target. This experiment, which has started taking data last year and has currently accumulated 2.29×10^{19} POT, seems to be confirming the $\nu_\mu \rightarrow \nu_\mu$ disappearance as expected by the atmospheric neutrino results [9].

The expected number of events in the FD can be computed as follows:

$$N_{\text{FD}} = R N_{\text{FD}}^{\text{theo}}, \quad (7)$$

where R is the ratio between the number of observed over the number of expected events in the Near Detector we have used the fact that $R \sim 0.84$ from Ref. [20], and $N_{\text{FD}}^{\text{theo}}$ is the theoretical expectation that can be calculated as

$$N_{\text{FD}}^{\text{theo}} = \eta n_{\text{FD}} \int \Phi_{\text{FD}}(E) \sigma(E) P(\nu_\mu \rightarrow \nu_\mu) dE, \quad (8)$$

where E is the neutrino energy, $\Phi_{\text{FD}}(E)$ is the ν_μ flux distribution at the Far Detector, $\sigma(E)$ is the total neutrino interaction cross section taken from Ref. [23], and n_{FD} is the number of active targets in the FD. Also, we have introduced a normalization factor η which was fixed to 0.65 in order to get the same expected number of ν_μ events as K2K for null oscillation. The shape of $\Phi_{\text{FD}}(E)$ was taken from Ref. [11], but the total flux has been renormalized to account for the number quoted in Table 1 of Ref. [20]. The survival probability $P(\nu_\mu \rightarrow \nu_\mu) = 1 - P(\nu_\mu \rightarrow \nu_\tau)$ in two generations, with $P(\nu_\mu \rightarrow \nu_\tau)$ either equal to zero (for no $\nu_\mu \rightarrow \nu_\tau$ conversion), to the usual two-generation MIO probability [Eq. (4)] or the PDM flavor conversion probability [Eq. (5)].

We first perform the calculation of the total number of expected events, N_{FD} , in the absence of any flavor change and for oscillation with $\sin^2 2\theta = 1$ and $\Delta m^2 = 3 \times 10^{-3} \text{ eV}^2$, $5 \times 10^{-3} \text{ eV}^2$, and $7 \times 10^{-3} \text{ eV}^2$ for 2.29×10^{19} POT. These results, which agree quite well with the K2K estimations presented in Ref. [4], are summarized in Table I. Thus we are confident that our numbers are reason-

TABLE I. Expected number of ν_μ events calculated for the K2K Far Detector of 22.5 kton. In all cases $\sin^2 2\theta = 1$.

Hypothesis	N_{FD}	Number of POT
No flavor change	40.3	2.29×10^{19}
$\Delta m^2 = 3 \times 10^{-3} \text{ eV}^2$	28.3	
$\Delta m^2 = 5 \times 10^{-3} \text{ eV}^2$	18.9	
$\Delta m^2 = 7 \times 10^{-3} \text{ eV}^2$	13.3	
$\Delta m^2 = 3 \times 10^{-3} \text{ eV}^2$	123	1.0×10^{20}
$\gamma_0 = 0.6 \times 10^{-21} \text{ GeV}$	122	

able and we can proceed to estimate the total number of events expected in the FD when K2K reaches 10^{20} POT for vacuum oscillation and decoherence. These numbers are also reported in Table I. From this, we can see that the mass induced oscillation and the decoherence effect at their best-fit values imply, for the goal of the K2K experiment, values for the total number of ν_μ events which are statistically compatible; hence the two solutions will be indistinct at K2K.

One may wonder about the energy distribution of the K2K events, which, in principle, could be used to discriminate the solutions. We show, in Fig. 1, the Monte Carlo simulated reconstructed neutrino spectrum for one-ring μ -like events at SuperK taken from Ref. [21] for $\Delta m^2 = 0.0015 \text{ eV}^2$, 0.0028 eV^2 , 0.005 eV^2 , and 0.01 eV^2 and $\sin^2 2\theta = 1$, as well as our estimation of the distortion ex-

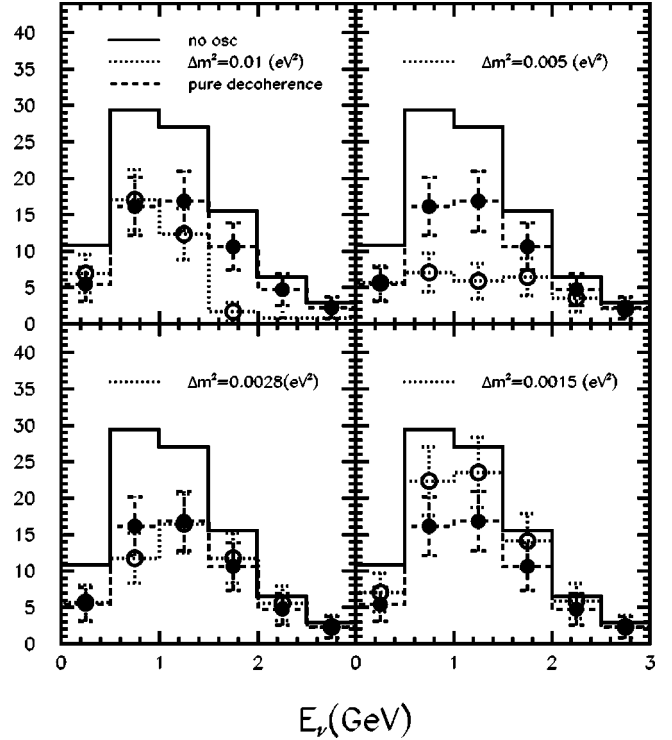


FIG. 1. Spectral distortion expected for one ring μ -like events at K2K assuming $\nu_\mu \rightarrow \nu_\tau$ flavor conversion with $\sin^2 2\theta = 1$ and different values of Δm^2 (MIO) and $\gamma_0 = 0.6 \times 10^{-21} \text{ GeV}$ (PDM). The bars represent the statistical error at each bin. The calculation was done for a total of 10^{20} POT.

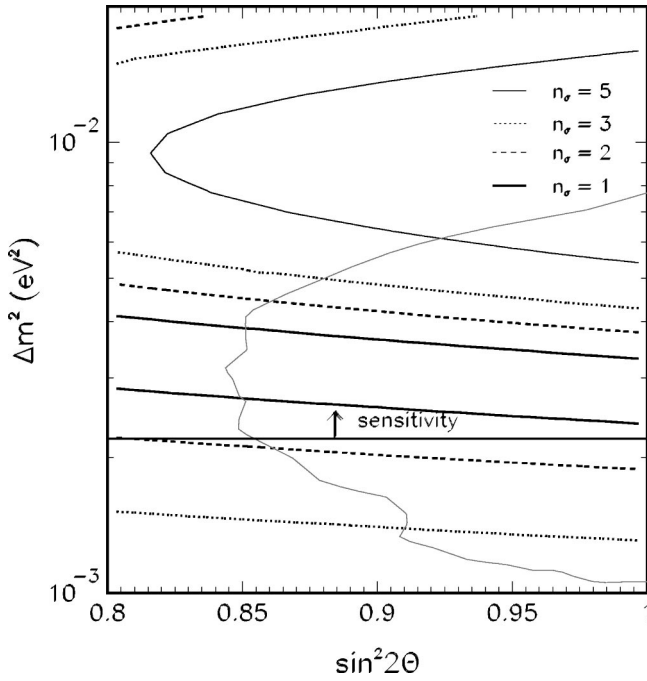


FIG. 2. Regions in the $\sin^2 2\theta \times \Delta m^2$ plane, for $\gamma_0 = \gamma_0^{\text{best}}$, where the numbers of N_{FD} events expected for PDM and MIO are separated by $n_\sigma = 1, 2, 3,$ and 5 for K2K after 10^{20} POT. The inner part of the gray curve is the one allowed at 99% C.L. by the latest SuperK atmospheric neutrino data [9]. The sensitivity of K2K is marked by a horizontal line with an arrow.

pected for the best-fit point of the PDM solution to the ANP. The latter was done simply by multiplying the bin content for no oscillation by the average PDM survival probability in the bin.

From Fig. 1, we see that if one takes into account only the statistic error, completely disregarding the systematic one, the curves are already virtually indistinguishable so that one unfortunately can hardly hope to discriminate between these two solutions with the K2K data. It is important to remark that the actual spectrum is currently under study, so what we present here can be viewed as a tendency which indicates that, even if one compares only the shape for the best-fit values of the two solutions, this type of discrimination will be very difficult in K2K.

In Figs. 2 and 3, we show the result of the statistical significance tests for K2K, as proposed in Sec. III. These curves were calculated with the total number of events, N_{FD} , and although this is not directly related to what is plotted in Fig. 1, it takes us basically to the same conclusion; i.e., for data compatible with $2.2 \times 10^{-3} \text{ eV}^2 \leq \Delta m^2 \leq 4.0 \times 10^{-3} \text{ eV}^2$ the maximal separation between the two solutions cannot exceed $\sim 2 \sigma$ if $\gamma_0 = \gamma_0^{\text{best}}$. We see in Fig. 3 that for data consistent with $2.2 \times 10^{-3} \text{ eV}^2 \leq \Delta m^2 \leq 3.5 \times 10^{-3} \text{ eV}^2$ the separation is always less than 3σ , $\forall \gamma_0$. A separation of 5 or more σ can only be achieved if the data are compatible with $\Delta m^2 \geq 7 \times 10^{-3} \text{ eV}^2$. We also see that the point which corresponds to the best fit of the MIO and the PDM solutions is inside the $n_\sigma \leq 1$ region. Therefore, we conclude that it will

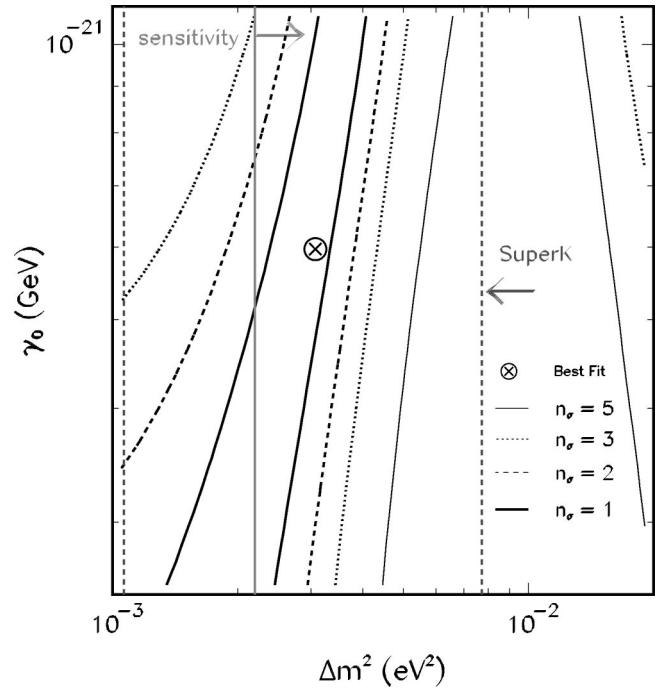


FIG. 3. Regions in the $\gamma_0 \times \Delta m^2$ plane, with $\sin^2 2\theta = 1$, where the numbers of N_{FD} events expected for PDM and MIO are separated by $n_\sigma = 1, 2, 3,$ and 5 for K2K after 10^{20} POT. The dotted gray lines mark the region allowed at 99% C.L. by the latest SuperK atmospheric neutrino data [9] and the cross the best-fit values of the PDM [8] and the MIO [9] solutions to the ANP. The start of the sensitivity of K2K is marked by an arrow.

be rather difficult to disentangle the two ANP solutions before the arrival of the next generation neutrino experiments.

B. MINOS

The MINOS experiment [12] is part of the Fermilab NuMI Project. The neutrinos which constitute the MINOS beam will be the result of the decay of pions and kaons that will be produced by the 120 GeV proton high intensity beam extracted from the Fermilab Main Injector. There will be two MINOS detectors, one located at Fermilab (the near detector) and another located in the Soudan mine in Minnesota, about 732 km away (the far detector of 5.4 kton).

According to Ref. [24], MINOS will be able to measure independently the rates and the energy spectra for muonless (0μ) and single muon (1μ) events, which are related to the neutral current (nc) and charged current (cc) reactions. Three different neutrino energy regions are possible: low ($E_\nu \sim 3 \text{ GeV}$), medium ($E_\nu \sim 7 \text{ GeV}$), and high ($E_\nu \sim 15 \text{ GeV}$). For MINOS to operate as a ν_τ appearance experiment either the high or medium energy beam is required, since one must be above the τ threshold of 3.1 GeV.

We have studied here two different observables that can be measured in MINOS: the 1μ -event energy spectrum and the $0\mu/1\mu$ -event ratio. The three different beam possibilities were investigated.

The expected number of 1μ events in MINOS, $dN_{1\mu}$, can be calculated using [25]

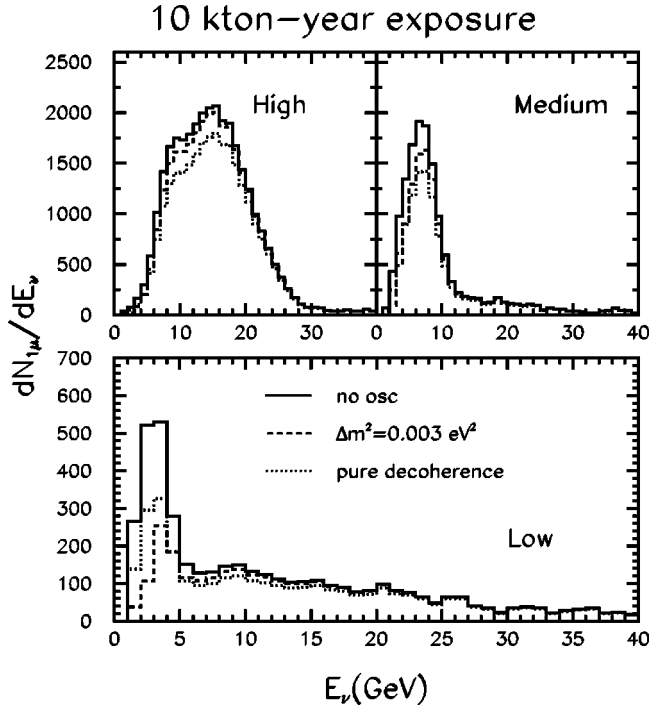


FIG. 4. Spectral distortion expected at MINOS for the best-fit points of the vacuum oscillation and of the pure decoherence solutions to the ANP for three possible beam configurations.

$$\frac{dN_{1\mu}}{dE_\nu}(E_\nu) = \frac{dN_{cc}}{dE_\nu}(E_\nu) \{ [1 - P(\nu_\mu \rightarrow \nu_\tau)] + P(\nu_\mu \rightarrow \nu_\tau) \eta(E_\nu) \text{Br}(\tau \rightarrow \mu) \}, \quad (9)$$

where $\eta(E_\nu) = \sigma_{\nu_\tau - cc}(E_\nu) / \sigma_{\nu_\mu - cc}(E_\nu)$ is the ratio of the cc cross section for ν_τ over the cc cross section for ν_μ , $\text{Br}(\tau \rightarrow \mu)$ is the branching ratio of the tau leptonic decay to muon (18%), dN_{cc}/dE_ν is the energy spectrum for ν_μ cc events in the MINOS far detector in the case of no flavor change [24], and $P(\nu_\mu \rightarrow \nu_\tau)$ is the probability of $\nu_\mu \rightarrow \nu_\tau$ conversion.

There are two different ways a muon can be produced: either by the surviving ν_μ which interact with the detector [first term of Eq. (9)] or by the contribution from taus generated by ν_τ interactions in the detector, after $\nu_\mu \rightarrow \nu_\tau$ conversion, followed by $\tau \rightarrow \nu_\mu \nu_\tau \mu$ decay [second term of Eq. (9)]. In both cases, the events must trigger the detector and be identified as muons to count as 1μ events. Here, we have not considered the possible contamination from neutral current events and the trigger and identification efficiencies were supposed to be 100%.

In Fig. 4, we present the 1μ -event energy distribution expected at MINOS for no flavor change and the best-fit parameters of the MIO and of the PDM solutions to the ANP for 10 kton year (~ 2 years of running). We can observe that if the final choice of beam is the low energy configuration, MINOS will be in the same footing of K2K, meaning that discrimination between solutions will be extremely disfavored due to low statistics. In the event of a choice fall on the medium or the high energy beam, discrimination will become more likely due to higher statistics.

We show in Fig. 5 the result of the statistical significance test in the $\Delta m^2 \times \sin^2 2\theta$ plane, for the three beam setups. We see that for $\Delta m^2 = 3 \times 10^{-3} \text{ eV}^2$, PDM and MIO are separated by less than 2σ (low), more than 3σ (medium), and more than 5σ (high), $\forall \sin^2 2\theta$ in the range compatible with SuperK atmospheric data, confirming our previous conclusions on Fig. 4.

We can further point out that, considering the 99% C.L. $\sin^2 2\theta \times \Delta m^2$ region allowed by the SuperK data [9], the two solutions will be indistinguishable within 3σ for $1.7 \times 10^{-3} \text{ eV}^2 \leq \Delta m^2 \leq 5.3 \times 10^{-3} \text{ eV}^2$ in the low energy configuration, for $3.0 \times 10^{-3} \text{ eV}^2 \leq \Delta m^2 \leq 4.3 \times 10^{-3} \text{ eV}^2$ in the medium energy configuration, and for $4.2 \times 10^{-3} \text{ eV}^2 \leq \Delta m^2 \leq 6.2 \times 10^{-3} \text{ eV}^2$ in the high energy configuration.

In Fig. 6, we show the statistical significance test in the plane $\gamma_0 \times \Delta m^2$ for the three energy possibilities. The point which corresponds to the best fit of the MIO and the PDM solutions is inside the $n_\sigma \leq 1$ region for low, the $n_\sigma \leq 2$ re-

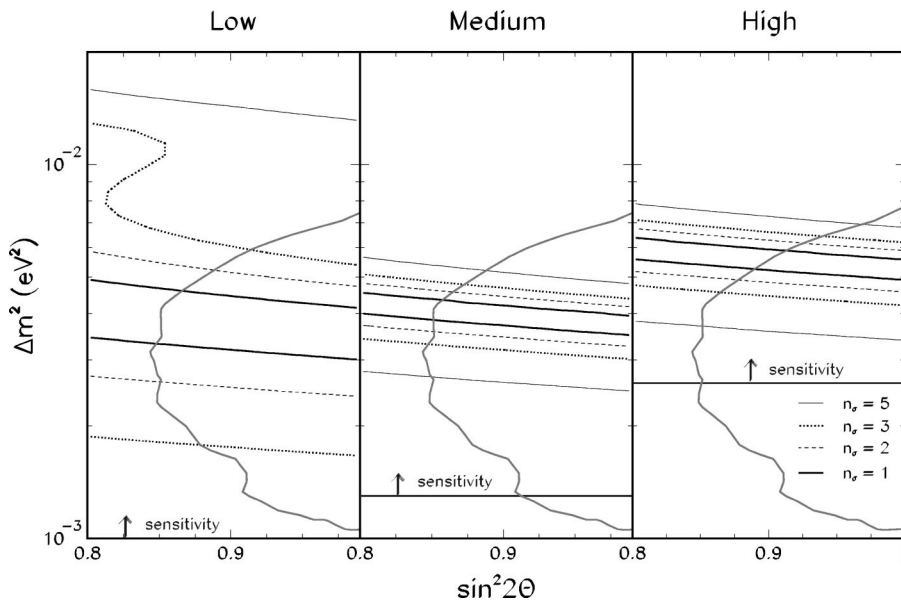


FIG. 5. Same as Fig. 2 but for $N_{1\mu}$ events in MINOS after 10 kton year exposure. The sensitivity of MINOS is marked by a horizontal line with an arrow.

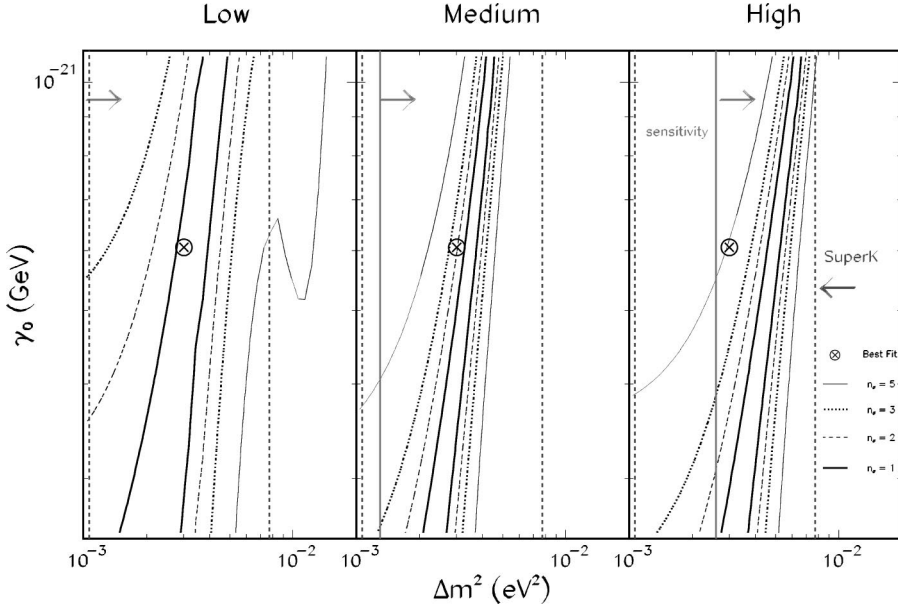


FIG. 6. Same as Fig. 3 but for $N_{1\mu}$ events in MINOS after 10 kton year exposure. The sensitivity of MINOS is marked by a vertical solid line with an arrow.

gion for medium, and only for the high energy case it falls into the $n_\sigma \geq 5$ region. Here it is again demonstrated that the medium and high energy setups are preferable to the low one if the issue is to discriminate the two mechanisms.

We have also computed the ratio $R_{0\mu/1\mu}$ that should be expected in MINOS as a function of the free parameters of the flavor changing hypothesis. This ratio has the advantage that it does not require understanding of the relative fluxes at the near and far detectors; it is also quite sensitive to neutrino flavor conversion since when they occur not only are 1μ events depleted but 0μ events are enhanced. This ratio can be written as [25]

$$R_{0\mu/1\mu} = \frac{\int dN_{0\mu}(E_\nu)}{\int dN_{1\mu}(E_\nu)}. \quad (10)$$

The number of expected 0μ events can be calculated as

$$\frac{dN_{0\mu}}{dE_\nu}(E_\nu) = \left[\frac{dN_{nc}}{dE_\nu}(E_\nu) + \frac{dN_{cc}}{dE_\nu}(E_\nu) P(\nu_\mu \rightarrow \nu_\tau) \eta(E_\nu) \right] \times [1 - \text{Br}(\tau \rightarrow \mu)]. \quad (11)$$

where we again supposed no contamination and the trigger and identification efficiencies to be 100%. We can infer dN_{nc}/dE_ν , the expected energy spectrum for ν_μ nc events in the MINOS far detector in the case of no flavor change, using the approximation

$$\frac{dN_{nc}}{dE_\nu}(E_\nu) \sim \frac{dN_{cc}}{dE_\nu}(E_\nu) \frac{\sigma_{\nu_\mu\text{-nc}}(E_\nu)}{\sigma_{\nu_\mu\text{-cc}}(E_\nu)}. \quad (12)$$

The cross sections $\sigma_{\nu_\mu\text{-cc}}$, $\sigma_{\nu_\tau\text{-cc}}$ were taken from Ref. [26] and $\sigma_{\nu_\mu\text{-nc}}$ from Ref. [23].

In Table II, we show our estimation of this ratio for no $\nu_\mu \rightarrow \nu_\tau$ conversion, mass induced oscillation for several values of Δm^2 , and PDM with $\gamma_0 = \gamma_0^{\text{best}}$ for the medium and high energy beams. For the low energy beam this test is ineffective since, in this case, MINOS will work essentially like a ν_μ disappearance experiment. For the medium and high energy beams, the ratios predicted for the best-fit values of the parameters of the two solutions seem to be well separated. Nevertheless, one has to take these results carefully; in a real experimental situation, experimental efficiencies, event contamination, resolution, and systematic errors can substantially affect 0μ -event observables.

TABLE II. Expected ratio $R_{0\mu/1\mu}$ in MINOS for 10 kton per year exposure. The error is only statistical. In all cases $\sin^2 2\theta = 1$.

Medium energy beam	
Hypothesis	$R_{0\mu/1\mu}$
No flavor change	0.33 ± 0.01
$\Delta m^2 = 1.5 \times 10^{-3} \text{ eV}^2$	0.35 ± 0.01
$\Delta m^2 = 3.0 \times 10^{-3} \text{ eV}^2$	0.41 ± 0.01
$\Delta m^2 = 4.5 \times 10^{-3} \text{ eV}^2$	0.52 ± 0.01
$\Delta m^2 = 6.0 \times 10^{-3} \text{ eV}^2$	0.71 ± 0.01
$\gamma_0 = 0.6 \times 10^{-21} \text{ GeV}$	0.47 ± 0.01
High energy beam	
Hypothesis	$R_{0\mu/1\mu}$
No flavor change	0.314 ± 0.004
$\Delta m^2 = 1.5 \times 10^{-3} \text{ eV}^2$	0.320 ± 0.004
$\Delta m^2 = 3.0 \times 10^{-3} \text{ eV}^2$	0.340 ± 0.004
$\Delta m^2 = 4.5 \times 10^{-3} \text{ eV}^2$	0.380 ± 0.005
$\Delta m^2 = 6.0 \times 10^{-3} \text{ eV}^2$	0.430 ± 0.005
$\gamma_0 = 0.6 \times 10^{-21} \text{ GeV}$	0.413 ± 0.005

C. CERN to Gran Sasso neutrino oscillation experiments

The new CERN neutrino beam to Gran Sasso is a facility that will direct a ν_μ beam to the Gran Sasso Laboratory in Italy at 732 km from CERN. Such a beam together with the massive detectors ICANOE or OPERA [22] in Gran Sasso will constitute a powerful tool for long-base-line neutrino oscillation searches. The number of protons on target is expected to be 4.5×10^{19} per year, the ν_μ beam will have an average energy of 17 GeV, the fractions ν_e/ν_μ , ν_μ^-/ν_μ , and ν_τ/ν_μ in the beam are expected to be as low as 0.8%, 2%, and 10^{-7} , respectively [27]. The number of ν_μ charged current events per protons on target and kton, without neutrino oscillations, is calculated to be 4.7×10^{-17} for $1 \text{ GeV} \leq E_\nu \leq 30 \text{ GeV}$ [27]. These experiments are supposed to start taking data around 2005 and may be used to try to distinguish the two ANP solutions.

We have investigated the capability of these detectors, in particular OPERA, working in the $\nu_\mu \rightarrow \nu_\tau$ appearance mode, to elucidate which is the correct solution to the ANP. We have obtained the expected number of ν_τ events, N_τ , that will be measured by OPERA, considering a pure ν_μ beam, using the following expression:

$$N_\tau = A \int \phi_{\nu_\mu}(E) P(\nu_\mu \rightarrow \nu_\tau) \sum_{i=l,h} \text{Br}(\tau \rightarrow i) \times \sigma_{\nu_\tau\text{-cc}}(E) \epsilon_i(E) dE, \quad (13)$$

where ϕ_{ν_μ} is the flux of ν_μ at the Gran Sasso detector and $\sigma_{\nu_\tau\text{-cc}}$ is the charged current cross section for ν_τ , both taken from Ref. [26]. The number of active targets A can be calculated as $A = C_n \times M_d \times N_A \times 10^9 \times N_p \times N_y$ where M_d is the detector mass in kton, $N_A \times 10^9$ is the number of nucleons per kton (where $N_A = 6.02 \times 10^{23}$ is Avogadro's number), N_y is the number of years of data taking, N_p is the number of protons on target per year, and $C_n = 0.879$ is a normalization constant that we need to introduce in order to be able to reproduce the numbers presented in Table 27 of Ref. [13]. We have assumed that ν_τ identification will be accomplished through its one-prong decays into leptons (l) and hadrons (h). We have used the overall value $\sum_{i=l,h} \text{Br}(\tau \rightarrow i) \epsilon_i(E) = 8.7\%$, admitting a total mass of 2 kton for 5 yr of exposure, according to Ref. [13]. The probability $P(\nu_\mu \rightarrow \nu_\tau)$ is supposed to be equal either to zero (for no flavor transformation), to the MIO probability [Eq. (4)], or to the PDM probability [Eq. (5)].

In Table III, we show the number of ν_τ events we have calculated, according to Eq. (13), for a 5 yr exposure, assuming $\sin^2 2\theta = 1$ and four different values of Δm^2 and the best-fit point of the decoherence solution to the ANP. We also quote in this table the total number of background events, which remains after all the kinematical cuts have been applied, normalized to an exposure of 5 yr, taken from Ref. [13]. We observe that for the decoherence effect the rate of tau events is substantially higher than that of most of the Δm^2 hypotheses and higher than the number of background events.

We show in Fig. 7 the calculated energy spectrum for

TABLE III. Expected number of ν_τ events calculated for OPERA assuming a 5 yr exposure, using 8.7% for the total τ selection efficiency. In all MIO cases $\sin^2 2\theta = 1$.

Hypothesis	N_τ
$\Delta m^2 = 1.5 \times 10^{-3} \text{ eV}^2$	4
$\Delta m^2 = 3.0 \times 10^{-3} \text{ eV}^2$	16
$\Delta m^2 = 4.5 \times 10^{-3} \text{ eV}^2$	36
$\Delta m^2 = 6.0 \times 10^{-3} \text{ eV}^2$	62
$\gamma_0 = 0.6 \times 10^{-21} \text{ GeV}$	69
Total background ~ 0.6 events [13]	

both flavor changing scenarios at OPERA for 5 yr exposure, this was calculated using Eq. (13). In spite of the fact that in some cases we observe that the ratio between the number of ν_τ events coming from the PDM and MIOs is higher than 4, in practice, it seems to be very difficult to observe this difference due to low statistics.

In Fig. 8, we show the result of the first statistical significance test. From this we see that discrimination between the PDM and MIOs can become difficult if $\Delta m^2 \gtrsim 4.4 \times 10^{-3} \text{ eV}^2$ ($n_\sigma \leq 5$).

It is worth mentioning that if we vary the decoherence parameter in the range $0.25 \times 10^{-21} \text{ GeV} \leq \gamma_0 \leq 1.1 \times 10^{-21} \text{ GeV}$, the number of expected N_τ events also varies from 31 to 114. This suggests that there might be

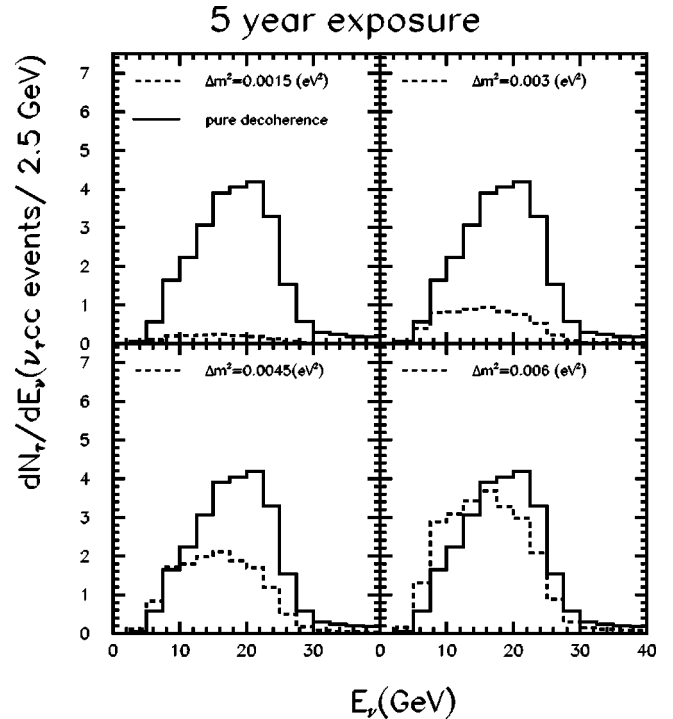


FIG. 7. Spectral distortion expected at OPERA for different values of Δm^2 (dashed lines) as well as for the best-fit point of the pure decoherence (solid line) solution to the ANP, for a 5 yr exposure. We have taken into account an overall efficiency of 8.7% in accordance with Ref. [13]. In all cases $\sin^2 2\theta = 1$.

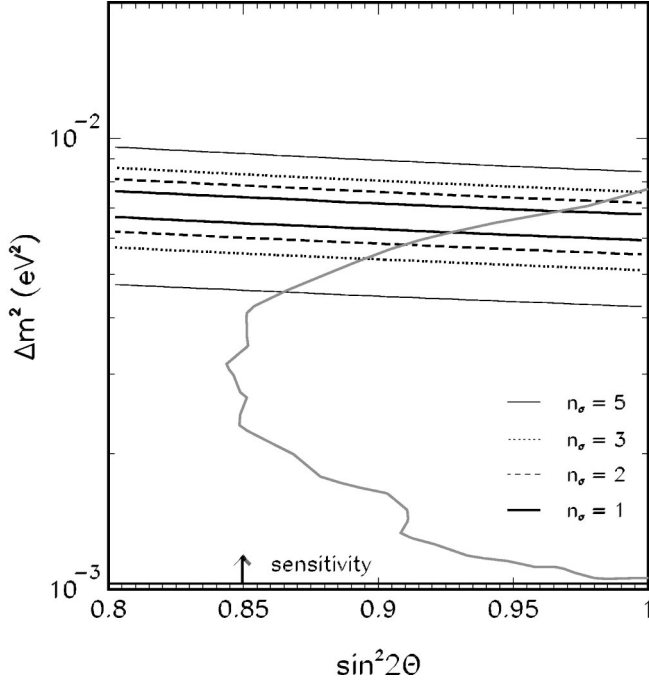


FIG. 8. Same as Fig. 2 but for N_τ events in OPERA after 5 years. The sensitivity of OPERA is marked by an horizontal line with an arrow.

some situations, even if the measured number of events is consistent with $\Delta m^2 \lesssim 4.4 \times 10^{-3} \text{ eV}^2$, where it might be difficult to disentangle the two ANP solutions in OPERA. This becomes clearer in Fig. 9, where we see that for data compatible with $\Delta m^2 < 4.1 \times 10^{-3} \text{ eV}^2$ a separation of more than 3σ can be achieved for $\gamma_0 \gtrsim 4 \times 10^{-21} \text{ GeV}$, but data consis-

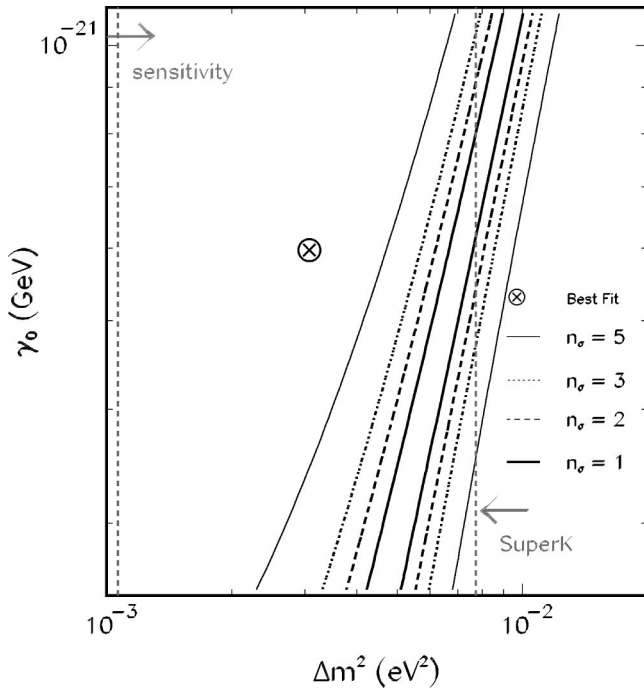


FIG. 9. Same as Fig. 3 but for N_τ events in OPERA after 5 years. The sensitivity of OPERA is marked by an arrow.

tent with values of $\Delta m^2 \sim 5.3 \times 10^{-3} \text{ eV}^2$ can only be separated from the PDM solution if $\gamma_0 \gtrsim 7 \times 10^{-21} \text{ GeV}$ ($n_\sigma \gtrsim 5$).

D. Neutrino factory in a muon collider

Many authors [14,28,29] have emphasized the advantages of using the straight section of a high intensity muon storage ring to make a neutrino factory. The muons (antimuons) accelerated to an energy E_μ ($E_{\bar{\mu}}$) constitute a pure source of both ν_μ ($\bar{\nu}_\mu$) and $\bar{\nu}_e$ (ν_e) through their decay $\mu^- \rightarrow e^- \bar{\nu}_e \nu_\mu$ ($\mu^+ \rightarrow e^+ \nu_e \bar{\nu}_\mu$) with well-known initial flux and energy distribution.

In the many propositions for this type of long-base-line neutrino factory one can find in the literature, the stored muon (antimuon) energy E_μ ($E_{\bar{\mu}}$) ranges from 10 GeV to 250 GeV and the neutrino beam is directed towards a far-away detector at a distance corresponding to an oscillation base line L varying from 730 km to 10 000 km.

Here we have explored the neutrino factory as a disappearance $\nu_\mu \rightarrow \nu_\mu$ experiment. We will explicitly discuss the case when negative muons are stored in the ring; a similar calculation can be performed when positive muons are the ones which decay producing neutrinos. The relevant observable is the total number of μ that can be detected when μ is the produced charged lepton in the beam, i.e., the number of ‘‘same sign muons’’ that we will denote here by N_μ . We define N_μ , for unpolarized muons (see the Appendix), as

$$N_\mu = n_\mu M_d \frac{10^9 N_A E_\mu^3}{m_\mu^2 \pi L^2} \int_{E_{\text{th}}/E_\mu}^1 h_0(x) \epsilon_\mu(x E_\mu) \times \left\{ \frac{\sigma_{\nu_\mu\text{-cc}}(x E_\mu)}{E_\mu} [1 - P(\nu_\mu \rightarrow \nu_\tau)] + \frac{\sigma_{\nu_\tau\text{-cc}}(x E_\mu)}{E_\mu} \right. \\ \left. \times \text{Br}(\tau \rightarrow \mu) P(\nu_\mu \rightarrow \nu_\tau) \right\} dx, \quad (14)$$

where E_μ is the muon source energy, $x = E_\nu/E_\mu$, M_d is the detector mass in ktons, n_μ number of useful μ decays, $10^9 N_A$ is the number of nucleons in 1 kton, and m_μ is the mass of the muon. The function h_0 contains the ν_μ energy spectrum normalized to 1 explicitly given in the Appendix. The charged current interaction cross sections per nucleon, $\sigma_{\nu_\mu\text{-cc}}$ and $\sigma_{\nu_\tau\text{-cc}}$, can be found in Ref. [26]. This number has two contributions, one from the ν_μ produced in the decay that survive and arrive at the detector interacting with it producing a final μ , another from the ν_τ that are produced by the flavor conversion mechanism and interact in the detector via charge current producing τ , which subsequently decays to μ with a branching ratio $\text{Br}(\tau \rightarrow \mu)$. We have calculated the above integral from $E_{\text{th}} = 3 \text{ GeV}$ to ensure good detection efficiency [31], so that we can consider the μ detection efficiency ϵ_μ to be 100%, independent of energy.

The muon beam is expected to have an average angular divergence of $\mathcal{O}(0.1 m_\mu/E_\mu)$. It was pointed out in Ref. [29] that this effect is about 10%, so we have multiplied our calculated number of events by 0.9 to account for this. The

TABLE IV. Expected number of μ events, N_μ , for a few configurations of a neutrino factory under the three studied hypotheses. Scenario (1) corresponds to a total of 1.6×10^{20} μ decays per year and a 10 kton detector, scenario (2) to a total of 2.0×10^{20} μ decays per year and a 40 kton detector. The numbers in scenario (1) are calculated for 1 year while in scenario (2) are for 5 years of data taking. The errors given are only statistical. For MIO we used $\sin^2 2\theta=1$.

Hypothesis	N_μ (1)			N_μ (2)		
L (km)	3096	6192	9289	3096	6192	9289
E_μ (GeV)	10	20	30	10	20	30
No flavor change	1315 ± 36	2580 ± 50	3804 ± 61	32880 ± 181	64501 ± 253	95101 ± 308
$\Delta m^2 = 3 \times 10^{-3}$ eV ²	222 ± 15	503 ± 22	805 ± 28	5554 ± 75	12596 ± 112	20141 ± 141
$\gamma_0 = 0.6 \times 10^{-21}$ GeV	716 ± 27	1439 ± 37	2156 ± 46	17918 ± 134	35991 ± 189	53910 ± 232

contribution of the background to the number of muons observed in the detector, which includes muons from charm decays produced by charged current and neutral current interactions in the detector, has been neglected because this would be a small global contribution.

Since the final configuration of such a facility is still not defined, we have tried to estimate the optimum configuration in order to maximize the difference between the mass induced $\nu_\mu \rightarrow \nu_\mu$ survival probability and pure decoherence. As observed in Ref. [8], at the best-fit point of the MIO and PDM solutions, the argument of the cosine, in the MIO case, and the argument of the exponential, in the PDM case, can be viewed as approximately the same. Explicitly,

$$P(\nu_\mu \rightarrow \nu_\mu) \approx \frac{1}{2}[1 + \cos(X)] \quad (\text{MIO}), \quad (15)$$

$$P(\nu_\mu \rightarrow \nu_\mu) \approx \frac{1}{2}[1 + e^{-X}] \quad (\text{PDM}), \quad (16)$$

where

$$X = \beta \frac{L}{E_\nu}, \quad (17)$$

with $\beta = 2.54 \Delta m^2 \sim 1.0 \times 10^{19} \gamma_0$, Δm^2 given in eV², γ_0 in GeV, and β in GeV/km, so that we can maximize the difference between the probabilities simply by finding the values of X , which maximize the function

$$F(X) = |\cos(X) - e^{-X}|. \quad (18)$$

This means that one has to numerically solve for X the transcendental equation

$$e^{-X} - \sin(X) = 0, \quad (19)$$

with the condition $\cos(X) > -e^{-X}$.

Once we find the spectrum of solutions X we can apply Eq. (17) to find the optimal distance L_{opt} by choosing a value for E_μ and fixing E_ν at the average value of the observable neutrino energy, i.e. $\langle E_\nu \rangle = 0.7 E_\mu$ [30], with $\beta = 6.1 \times 10^{-3}$ GeV/km, the best-fit value of Ref. [8]. We have calculated the maximal difference between the two sur-

vival probabilities for $E_\mu = 10$ GeV, 20 GeV, 30 GeV, and 50 GeV as a function of L , but only kept the cases where this difference reaches about 50%. This was obtained for $L_{\text{opt}} = 3096$ km, 6192 km, and 9289 km and $E_\mu = 10$ GeV, 20 GeV, and 30 GeV, respectively.

Note that using these criteria, we are looking for a maximum in the absolute difference between the survival probabilities [$\mathcal{O}(0.5)$], which is a very strong condition that we impose in order to detect and distinguish the signal of the ν_μ disappearance. Since this depends on the number of muon decays, which is big, this ensures that the signal will be quite sizable experimentally. We have seen before (see for instance Fig. 7) that there are cases of L/E where the absolute difference in the survival probabilities is small while the ratio $P(\nu_\mu \rightarrow \nu_\tau)(\text{PDM})/P(\nu_\mu \rightarrow \nu_\tau)(\text{MIO})$ is big, but since the statistics is poor, this ratio is an ambiguous observable to establish the difference between the PDM and MIOs.

Using Eq. (14) we have estimated the neutrino event rate for the three different hypotheses: no flavor conversion, MIO, and PDM.

We addressed a few optimal configurations so that our conclusions may be useful in planning real experimental setups. For each optimal situation, we have performed our calculation for two possible scenarios: (1) a total of 1.6×10^{20} μ decays per year with a detector of 10 kton; (2) a total of 2.0×10^{20} μ decays per year with a detector of 40 kton. Since the event rate is proportional to E_μ^3/L^2 [see Eq. (14)], the most conservative configuration is the one with $L_{\text{opt}} = 3096$ km and $E_\mu = 10$ GeV. Our results are summarized in Table IV. It is clear that one can distinguish among all the studied hypotheses, even in the most modest scenario (1).

An even more conclusive result can be obtained by looking at the energy distribution dN_μ/dE_ν [see Eq. (A10)] for charged current μ events. We show, in Fig. 10, our predictions, for 5 years of data taking, assuming 2.0×10^{20} μ decays per year, $E_\mu = 10$ GeV, $L = 3096$ km for null oscillation, the best-fit point of the PDM solution to the ANP, and four different values of Δm^2 which are consistent with the MIO solution to the ANP. We see that in the majority of cases a distinct signal will be observed, making it possible to establish which of the flavor changing hypotheses is the correct one.

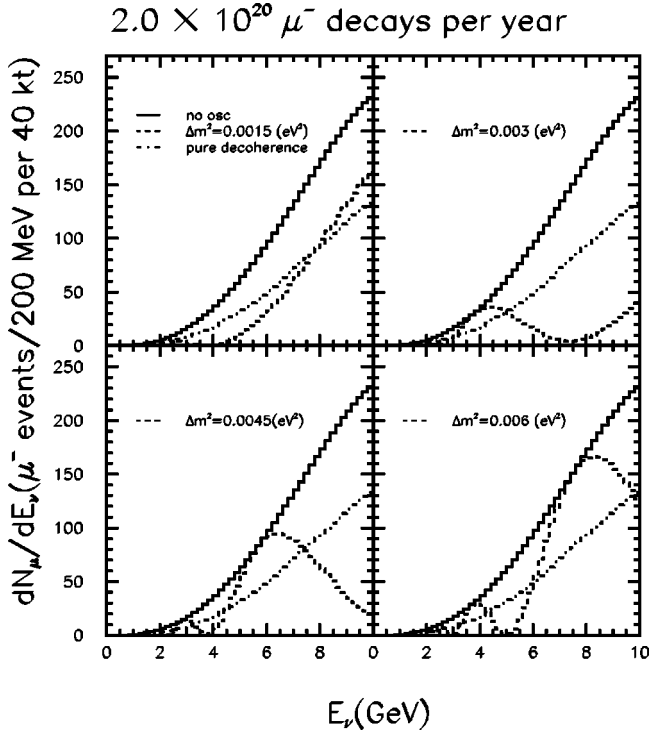


FIG. 10. Spectral distortion expected at a neutrino factory for $E_\mu = 10$ GeV, $L = 3096$ km, and several values of Δm^2 as well as for no flavor change (continuous line) and for the best-fit point of the pure decoherence (dot-dashed line) solution to the ANP, after 5 years of data taking. In all MIO cases $\sin^2 2\theta = 1$.

Although we have optimized the setup parameters in order to maximize the separation between the two ANP solutions at their best-fit point, we also have checked that even if we allow γ_0 to vary around the best-fit value, i.e. $0.25 \times 10^{-21} \text{ GeV} \leq \gamma_0 \leq 1.1 \times 10^{-21} \text{ GeV}$, we will get an energy spectrum which will always increase monotonically with neutrino energy. In this range these curves will all coincide up to 4 GeV; after that, if $\gamma_0 < 0.6 \times 10^{-21} \text{ GeV}$, the growth will be slightly slower than what is shown in Fig. 10 for $\gamma_0 = 0.6 \times 10^{-21} \text{ GeV}$, and if $\gamma_0 > 0.6 \times 10^{-21} \text{ GeV}$, the curves will be steeper, approaching the one for no flavor change.

In Fig. 11, we show the statistical significance test for 5 years of data taking in the plane $\Delta m^2 \times \sin^2 2\theta$ assuming the most conservative of optimal configurations. From this figure, we see that for most of the MIO parameter space the two solutions can be well discriminated. This conclusion is further confirmed by Fig. 12, where the statistical significance test was performed letting γ_0 vary. Here we note that for data compatible with $1.5 \times 10^{-3} \text{ eV}^2 \leq \Delta m^2 \leq 4.8 \times 10^{-3} \text{ eV}^2$ a very clear separation is possible $\forall \gamma_0$. It seems that unless the data prefer lower values of $\Delta m^2 \leq 1.5 \times 10^{-3} \text{ eV}^2$ or a few isolated islands in the plane $\gamma_0 \times \Delta m^2$, in which case a clear separation between the two solutions might be compromised, decoherence and mass induced oscillations will present a very distinct signature of their dynamics. Fortunately, for $\Delta m^2 \leq 1.5 \times 10^{-3} \text{ eV}^2$ and for $\Delta m^2 \geq 5.0 \times 10^{-3} \text{ eV}^2$ a clear-cut position between the two solutions can be accomplished respectively by the

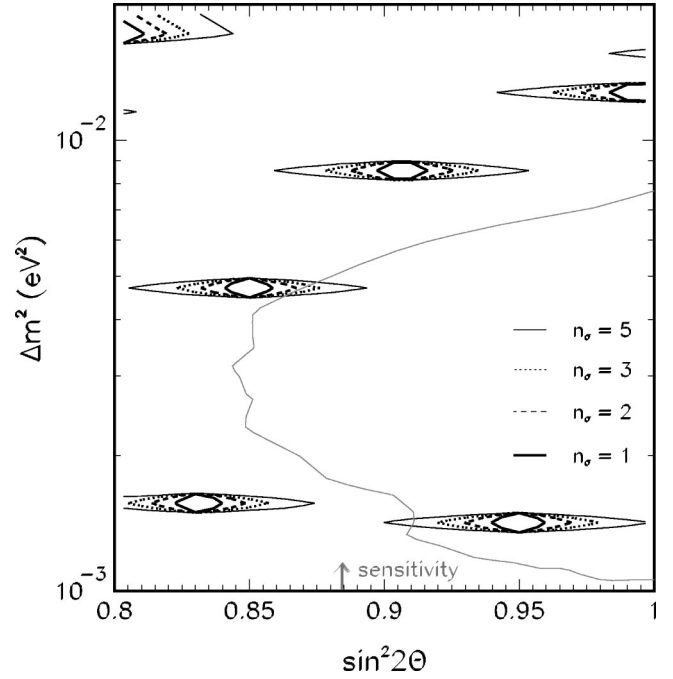


FIG. 11. Same as Fig. 2 but for N_μ events after 5 years of a neutrino factory in scenario (1) of Table IV. The sensitivity of this setup is marked by a horizontal line with an arrow.

OPERA and the MINOS (medium) experiments, as we have discussed in Secs. IV C and IV B.

V. CONCLUSIONS

We have discussed the perspectives of future experiments for distinguishing the MIO solution to the ANP from the

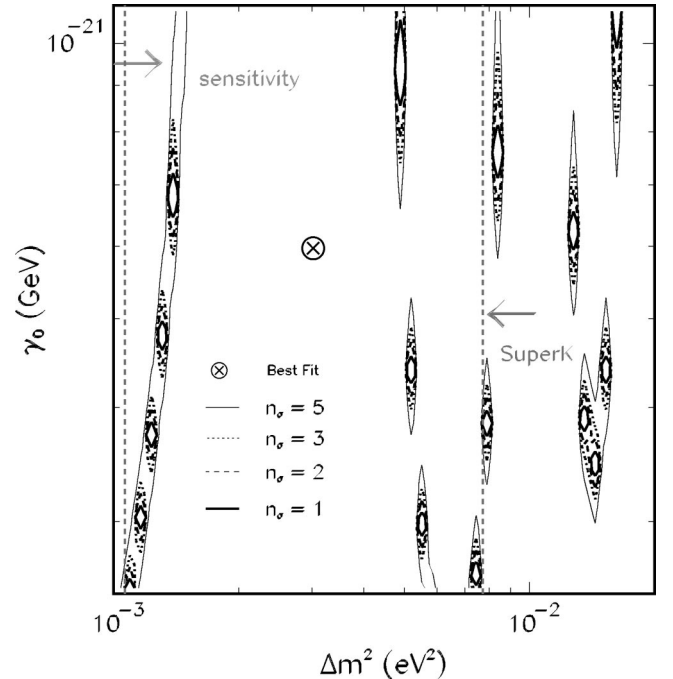


FIG. 12. Same as Fig. 3 but for N_μ events after 5 years of a neutrino factory in scenario (1) of Table IV. The start of the sensitivity of this setup is marked by an arrow.

PDM one. This is especially important since it will be very difficult for NOMAD and CHORUS to achieve a sensitivity in the $\nu_\mu \rightarrow \nu_\tau$ mode to directly exclude or confirm the latter solution [17].

Our study discriminating these two ANP solutions permitted us to arrive at the following general conclusions: K2K and probably MINOS will not be able to shed much light on the dynamics which promotes $\nu_\mu \rightarrow \nu_\tau$ conversion; OPERA and a neutrino factory in a muon collider are more suitable for this job.

From the statistical significance tests we have performed, considering positive discrimination only if $n_\sigma \geq 5$, we can say the following. K2K cannot discriminate PDM from MIO if the data are compatible with $2.2 \times 10^{-3} \text{ eV}^2 \leq \Delta m^2 \leq 4.5 \times 10^{-3} \text{ eV}^2$, $\forall \gamma_0$. In fact, this almost covers the entire parameter space allowed by the SuperK atmospheric data at 99% C.L., as can be seen in Fig. 2. MINOS, in the low energy beam configuration, cannot separate the two solutions if the data are compatible with $1.1 \times 10^{-3} \text{ eV}^2 \leq \Delta m^2 \leq 5.2 \times 10^{-3} \text{ eV}^2$, $\forall \gamma_0$; in the medium energy beam configuration, if $3.0 \times 10^{-3} \text{ eV}^2 \leq \Delta m^2 \leq 4.0 \times 10^{-3} \text{ eV}^2$, $\forall \gamma_0$; and in the high energy beam configuration, if $4.8 \times 10^{-3} \text{ eV}^2 \leq \Delta m^2 \leq 5.1 \times 10^{-3} \text{ eV}^2$, $\forall \gamma_0$. Running with the low energy setup, MINOS will be very similar to K2K, and certainly will not be able to discriminate solutions; see Figs. 5 and 6. For the high energy setup MINOS will be more selective and similar to OPERA. OPERA, after 5 years, will only not disentangle the PDM from MIOs if the data are compatible with $5.9 \times 10^{-3} \text{ eV}^2 \leq \Delta m^2 \leq 6.7 \times 10^{-3} \text{ eV}^2$, $\forall \gamma_0$. This corresponds to the upper corner of the SuperK 99% C.L. region; see Fig. 8. A neutrino factory with $E_\mu = 10 \text{ GeV}$, $L = 3096 \text{ km}$, and $1.6 \times 10^{20} \mu^-$ decays per year, with a detector of 10 kton after 5 years of data taking, will still not be able to discriminate the two solutions if the data prefer a small island in the plane $\sin^2 2\theta \times \Delta m^2$, at $\Delta m^2 \sim 1.5 \times 10^{-3} \text{ eV}^2$ and $\sin^2 2\theta \sim 0.95$; see Fig. 11. On the other hand, if the data are compatible with $1.5 \times 10^{-3} \text{ eV}^2 \leq \Delta m^2 \leq 5 \times 10^{-3} \text{ eV}^2$, the separation between the PDM and MIOs will be extremely clear, $\forall \gamma_0$. This type of facility, it seems, will be the only one able to measure spectral distortions and, thereby, directly test if neutrino flavor change is indeed an oscillation phenomenon.

In any case, combination of the results of all these proposed experiments will most certainly unravel the dynamics of neutrino conversion in the $\nu_\mu \rightarrow \nu_\tau$ mode if only active neutrinos exist in nature.

There is a proposed atmospheric neutrino experiment, MONOLITH [32], which, in principle, could distinguish the PDM from MIOs through observation of the first oscillation minimum. Here we have only investigated the capabilities of accelerator neutrino experiments which we believe have to be performed in order to completely ratify the mechanism behind neutrino flavor change.

ACKNOWLEDGMENTS

We thank GEFAN for valuable discussions and useful comments. This work was supported by Conselho Nacional de Desenvolvimento Científico e Tecnológico (CNPq) and

TABLE V. Flux functions $h_0(x)$ and $h_1(x)$.

$h_0(x)$	$h_1(x)$
$2x^2(3-2x)$	$2x^2(1-2x)$

by Fundação de Amparo à Pesquisa do Estado de São Paulo (FAPESP).

APPENDIX

The distribution of ν_μ in the decay $\mu^- \rightarrow e^- + \bar{\nu}_e + \nu_\mu$ in the muon rest frame (c.m.) is given by [14]

$$\frac{d^2 N_{\nu_\mu}}{dx d\Omega_{\text{c.m.}}} = \frac{1}{4\pi} [h_0(x) + \mathcal{P}_\mu h_1(x) \cos \theta_{\text{c.m.}}], \quad (\text{A1})$$

$x = 2E_\nu^{\text{c.m.}}/m_\mu$, where $E_\nu^{\text{c.m.}}$ denotes the neutrino energy, $\theta_{\text{c.m.}}$ is the angle between the neutrino momentum vector and the muon spin direction, and \mathcal{P}_μ is the average muon polarization along the beam directions. The functions h_0 and h_1 are given in Table V.

On applying a Lorentz transformation to boost the laboratory frame (lab), it is found that the neutrino energy distribution at any polar angle is just scaled by a relativistic boost factor depending on the angle

$$E_\nu^{\text{lab}} = \frac{1}{2} x E_\mu^{\text{lab}} (1 + \beta \cos \theta_{\text{c.m.}}) \quad (\text{A2})$$

and

$$\sin \theta_{\text{lab}} = \frac{\sin \theta_{\text{c.m.}}}{\gamma(1 + \beta \cos \theta_{\text{c.m.}})}, \quad (\text{A3})$$

where β and γ are the usual relativistic factors and we have used $\gamma = E_\mu^{\text{lab}}/m_\mu$.

Because in the long-base-line experiments only ν_μ emitted in the forward direction are relevant to the computed flux, one can make the following approximation: $\cos \theta_{\text{c.m.}} \approx 1$, $\sin \theta_{\text{c.m.}} \approx \theta_{\text{c.m.}}$. Also at high energy $\beta \approx 1$. Hence Eq. (A2) leads to $x = E_\nu^{\text{lab}}/E_\mu^{\text{lab}}$. Then, we can rewrite $d\Omega_{\text{c.m.}}$ in terms of $d\Omega_{\text{lab}}$ as

$$d\Omega_{\text{c.m.}} = \gamma^2 (1 + \beta)^2 d\Omega_{\text{lab}}. \quad (\text{A4})$$

Substituting Eq. (A4) into Eq. (A1), we obtain, as a function of the lab variables,

$$\frac{d^2 N_{\nu_\mu}}{dx d\Omega_{\text{lab}}} = \frac{(E_\mu^{\text{lab}})^2}{m_\mu^2 \pi} [h_0(x) \pm \mathcal{P}_\mu h_1(x) \cos \theta_{\text{c.m.}}], \quad (\text{A5})$$

which for unpolarized muons simplifies to

$$\frac{d^2 N_{\nu_\mu}}{dx d\Omega_{\text{lab}}} = \frac{(E_\mu^{\text{lab}})^2}{m_\mu^2 \pi} h_0(x) \rightarrow \frac{dN_{\nu_\mu}}{dE_\nu^{\text{lab}}} = 4\pi \frac{E_\mu^{\text{lab}}}{m_\mu^2 \pi} h_0(x). \quad (\text{A6})$$

The number of expected μ events from ν_μ interactions with the detector is given by

$$N_\mu \equiv \underbrace{n_\mu M_d 10^9 N_A}_{\text{normalization}} \times \Phi \times \sigma \times \epsilon_\mu. \quad (\text{A7})$$

The ν_μ flux Φ can be written as

$$\Phi = \frac{N_{\nu_\mu}}{4\pi L^2} \frac{1}{t} \rightarrow \frac{d\Phi}{dE_\nu^{\text{lab}}} = \frac{1}{4\pi L^2} \frac{1}{t} \frac{dN_{\nu_\mu}}{dE_\nu^{\text{lab}}}. \quad (\text{A8})$$

Substituting Eq. (A6) into Eq. (A8), we get

$$\frac{d\Phi}{dE_\nu^{\text{lab}}} = \frac{E_\mu^{\text{lab}}}{m_\mu^2 \pi L^2} \frac{1}{t} h_0(x). \quad (\text{A9})$$

Finally, after t years,

$$\frac{dN_\mu}{dE_\nu^{\text{lab}}} = \frac{n_\mu M_d 10^9 N_A}{m_\mu^2 \pi L^2} E_\mu^{\text{lab}} h_0(x) \times \sigma \times \epsilon_\mu. \quad (\text{A10})$$

-
- [1] Super-Kamiokande Collaboration, Y. Fukuda *et al.*, Phys. Rev. Lett. **81**, 1562 (1998).
- [2] Soudan-2 Collaboration, W. Anthony Mann, Nucl. Phys. B (Proc. Suppl.) **91**, 134 (2000).
- [3] F. Ronga for the MACRO Collaboration, Nucl. Phys. B (Proc. Suppl.) **87**, 135 (2000).
- [4] M. Sakuda for the K2K Collaboration, talk given at the XXX International Conference on High Energy Physics (ICHEP 2000), Osaka, Japan, 2000, transparencies available at <http://ichep2000.hep.sci.osaka-u.ac.jp/scan/0728/pa08/sakuda/index.html>
- [5] Z. Maki, M. Nakagawa, and S. Sakata, Prog. Theor. Phys. **28**, 870 (1962).
- [6] G. L. Fogli, E. Lisi, A. Marrone, and G. Scioscia, Phys. Rev. D **60**, 053006 (1999).
- [7] V. Barger, J. G. Learned, S. Pakvasa, and T. J. Weiler, Phys. Rev. Lett. **82**, 2640 (1999); V. Barger, J. G. Learned, P. Lipari, M. Lusignoli, S. Pakvasa, and T. J. Weiler, Phys. Lett. B **462**, 109 (1999).
- [8] E. Lisi, A. Marrone, and D. Montanino, Phys. Rev. Lett. **85**, 1166 (2000).
- [9] H. Sobel for the Super-Kamiokande Collaboration, Nucl. Phys. B (Proc. Suppl.) **91**, 127 (2001).
- [10] A. M. Gago, O. L. G. Peres, W. J. C. Teves, and R. Zukanovich Funchal (in preparation).
- [11] Y. Oyama for the K2K Collaboration, talk given at the YITP workshop on flavor physics, Kyoto, Japan, 1998, hep-ex/9803014.
- [12] Minos Collaboration, ‘‘Neutrino Oscillation Physics at Fermilab: The NuMI-MINOS Project,’’ Fermilab Report No. NuMI-L-375, 1998.
- [13] OPERA Collaboration, ‘‘An appearance experiment to search for $\nu_\mu \rightarrow \nu_\tau$ oscillation in the CNGS beam,’’ Report No. CERN/SPSC 2000-028, SPSC/P318, LNGS P25/2000, 2000.
- [14] S. Geer, Phys. Rev. D **57**, 6989 (1998); **59**, 039903 (1999).
- [15] F. Benatti and R. Floreanini, J. High Energy Phys. **02**, 32 (2000).
- [16] J. Ellis, J. S. Hagelin, D. V. Nanopoulos, and M. Srednicki, Nucl. Phys. **B241**, 381 (1984).
- [17] A. M. Gago, E. M. Santos, W. J. C. Teves, and R. Zukanovich Funchal, Phys. Rev. D **63**, 073001 (2001).
- [18] H. V. Klapdor-Kleingrothaus, H. Päs, and U. Sarkar, Eur. Phys. J. A **8**, 577 (2000).
- [19] Particle Data Group, D. E. Groom *et al.*, Eur. Phys. J. C **15**, 1 (2000).
- [20] Y. Oyama for the K2K Collaboration, talk given at the XXX-Vth Rencontres de Moriond ‘‘Electroweak interactions and unified theories,’’ Les Arc, France, 2000, hep-ex/0004015.
- [21] T. Ishida for the K2K Collaboration, hep-ex/0008047.
- [22] A. Rubbia for the ICANOE/OPERA Collaboration, Nucl. Phys. B (Proc. Suppl.) **91**, 223 (2001).
- [23] The charged and neutral current cross sections were taken from M. D. Messier, Ph.D. thesis, Boston University, 1999, available at <http://hep.bu.edu/~messier/thesis>
- [24] MINOS Collaboration, P. Adamson *et al.*, Fermilab Report No. NuMI-L-337, 1998.
- [25] Minos Collaboration, K. R. Langenbach and M. C. Goodman, Fermilab Report No. NuMI-L-75, 1995.
- [26] The charged current cross sections for ν_μ and ν_τ can be obtained in the form of a table from <http://www.cern.ch/NGS>
- [27] ICANOE Collaboration, ‘‘ICANOE, A proposal for a CERN-GS long baseline and atmospheric neutrino oscillation experiment,’’ Report No. INFN/AE-99-17, CERN/SPSC 99-25, SPSC/P314, 1999; see <http://pcnometh4.cern.ch/publications.html>
- [28] A. De Rujula, M. B. Gavela, and P. Hernandez, Nucl. Phys. **B547**, 21 (1999).
- [29] V. Barger, S. Geer, and K. Whisnant, Phys. Rev. D **61**, 053004 (2000).
- [30] V. Barger, S. Geer, R. Raja, and K. Whisnant, Phys. Rev. D **62**, 013004 (2000).
- [31] M. Freund, M. Lindner, S. T. Petcov, and A. Romanino, Nucl. Phys. **B578**, 27 (2000).
- [32] K. Hoepfner for the MONOLITH Collaboration, Nucl. Phys. B (Proc. Suppl.) **87**, 192 (2000).